

• 电气工程 •

DOI:10.12454/j.jsuese.202300913



本刊网刊

基于双端电流测量的电缆早期故障定位研究

孟鹏飞¹, 李腾飞¹, 王万岗^{2*}, 谢施君³, 周凯¹, 唐志荣¹

(1. 四川大学电气工程学院, 四川成都 610065; 2. 成都师范学院物理与工程技术学院, 四川成都 610130;
3. 国网四川省电力公司电力科学研究院, 四川成都 610041)

摘要:随着电缆服役时间的增加,亟需在永久故障产生前开展早期故障研究。针对传统早期故障定位中的阻抗法定位精度随故障距离的增加而减小,以及单端行波法易造成故障位置误判的问题,提出基于双端电流法的电缆早期故障定位方法。首先,给出电缆中行波信号的传输线模型,并基于电弧脉冲在电缆中的传输过程,分析基于双端电流测量的故障定位的原理。然后,采用加 Hanning 窗的伪魏格纳分布(PWVD)算法对信号进行时频分布计算,并使用时频互相关函数估计双端信号的时间延迟,实现对早期故障定位的计算。接着,在 PSCAD/EMTDC 仿真软件中搭建 10 kV 电缆的早期故障模型来验证本文方法的可行性,并研究不同噪声干扰对定位结果的影响,仿真结果表明,早期故障位置计算的相对误差为 0.57%,具有较高的定位精度,并且不同程度噪声对定位结果的影响较小。最后,搭建电缆早期故障实验测试平台,进一步验证故障定位方法的效果,实验结果表明,本文方法的故障位置的相对误差为 5.36%,方法具有可行性。本文提出的电缆早期故障的定位方法可使日常运维检修更精准、高效,对提高电力系统的安全稳定运行有重要意义。

关键词:电缆早期故障;行波定位;双端电流;伪魏格纳分布;时频互相关

中图分类号: TM93

文献标志码: A

文章编号: 2096-3246(2025)04-0269-09

电缆因其可靠性高、不易受环境影响以及维护工作量小的特点,被广泛应用于城市配电网中^[1]。但随着运行年限的增加,在长期电效应、热效应、地下潮气及环境应力等因素的综合影响下,电缆及其附件会不可避免地产生局部的绝缘缺陷,严重影响电力系统的安全稳定运行^[2-5]。

电缆的早期故障一般由局部的绝缘缺陷引起,属于一种自恢复的间歇性接地电弧故障,根据电弧维持时间的不同,可以分为半周波电弧故障和多周波电弧故障^[6-8]。早期故障通常发生在电压峰值处,随着电缆绝缘劣化程度的增加,其发生频次会逐渐增加,最终会引起绝缘的击穿,演变为电缆永久性故障^[9-10]。在电缆尚未形成永久性故障前对早期故障进行识别与定位,可以更高效、精准地完成维护检修工作,对电力系统的稳定可靠运行具有重要意义。

对于电缆早期故障的识别目前已有较多研究。例如:周正雄等^[11]使用双边累计和算法对电缆故障相进

行识别,并引入自适应神经网络对电流信号的谐波指数进行计算,通过谐波含量曲线的变化实现对早期故障的识别。汪颖等^[12]使用小波变换提取电流特征来构建卷积神经网络,并通过修正损失函数及自适应学习率的方法实现对电缆早期故障的准确识别。姚海燕等^[13]使用多尺度小波变换提取故障电流的特征量,并提出基于多特征的暂态电流复合判据,使用灰度关联分析对电缆早期故障进行识别。Liu 等^[14]将稀疏自编码器与深度置信网络相结合,基于神经网络强大的学习能力对各种电缆故障信号进行分类和识别。

对于电缆的早期故障定位研究也已有较多研究。例如:张建等^[15]以阻抗法为基础构建故障相的电路模型,并根据过渡电阻的纯电阻性质推导出电缆故障距离与线路总长的关系,实现对早期故障的定位。Zhang 等^[16]同样构建基于故障相的电路模型,并将故障距离估计与电弧模型参数估计相结合,通过不断搜索故障距离,以电弧公式作为评估函数来评估故障位置。但

收稿日期:2023-11-15 修回日期:2023-12-26 网络出版日期:2024-05-22

基金项目:国家自然科学基金青年基金项目(52107158)

作者简介:孟鹏飞(1992—),男,副研究员,博士。研究方向:电力设备监测等。E-mail: mpf@scu.edu.cn

*通信作者:王万岗,副教授, E-mail: wangwangang@foxmail.com

是,上述基于阻抗法的测试方案并未考虑衰减效应及色散效应对电弧传输的影响^[17-18],因此随着故障距离的增加,上述方案的定位精度会不断降低。束洪春等^[19]基于行波理论,在特征频带下运用 TT 算法,通过提取两行波波头传输至电缆首端的时间差对早期故障进行定位,但对行波分析时未考虑行波在其余缺陷位置的折反射,因此容易造成对故障位置的误判。

基于以上分析,本文提出基于双端电流测量的电缆早期故障定位方法。首先,给出电缆中电磁波传播的分布式参数模型,通过分析电弧脉冲在电缆中的传播过程及在缺陷位置的折反射现象,提出基于双端行波测量的电缆早期故障定位方法的原理。然后,针对时域信号因易受噪声干扰而影响定位精度的问题,提出从时频域角度进行信号分析,通过分析时频变换特点,使用加 Hanning 窗的 PWVD 算法对双端电流信号进行时频变换;并且,使用时频互相关函数计算电弧脉冲传输至电缆两端的时间延迟,实现对电缆早期故障的定位。通过仿真模拟及实验,验证了本文方法具有较高的定位精度。

1 双端电流法定位方法的基本原理

1.1 电缆的传输线模型

根据传输线理论^[20],高频电磁波在电缆中的传播应按分布式参数计算。电缆的分布式模型如图 1 所示,其中, R, L, G, C 分别为单位长度下电缆的电阻(Ω/m)、电感(H/m)、电导(S/m)及电容(F/m), Δl 为单位长度。

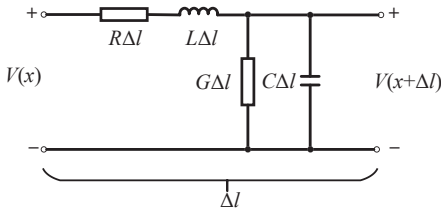


图1 电缆分布式参数模型

Fig. 1 Cable distributed parameter model

随着频率的增加,电缆的集肤效应及邻近效应逐渐加强,并改变介质中的电磁场分布,影响电缆的分布式参数^[21],各参数 R, L, G, C 的计算公式为:

$$\begin{cases} R \approx \frac{1}{2\pi} \sqrt{\frac{\mu_0 \omega}{2}} \left(\frac{1}{r_c} \sqrt{\rho_c} + \frac{1}{r_s} \sqrt{\rho_s} \right), \\ L \approx \frac{\mu_0}{2\pi} \ln \frac{r_s}{r_c} + \frac{1}{4\pi} \sqrt{\frac{2\mu_0}{\omega}} \left(\frac{1}{r_c} \sqrt{\rho_c} + \frac{1}{r_s} \sqrt{\rho_s} \right), \\ G = \frac{2\pi\sigma}{\ln(r_s/r_c)}, \\ C = \frac{2\pi\epsilon_r \epsilon_0}{\ln(r_s/r_c)} \end{cases} \quad (1)$$

式中: ω 为信号的角频率, $\omega=2\pi f$, f 为信号频率; μ_0 为真

空磁导率; r_c 和 r_s 分别为导体线芯半径及铜屏蔽层的内径; ρ_c 和 ρ_s 分别为线芯和屏蔽层的电阻率; σ 为绝缘介质的电导率; ϵ_r, ϵ_0 分别为相对介电常数、真空介电常数。

在以分布式模型计算电磁波的传播特性时,正弦稳态条件下电缆任意位置 x 处的电压及电流方程为:

$$\begin{cases} U(l) = U_i e^{-\gamma x} + U_r e^{\gamma x}, \\ I(l) = \frac{1}{Z_0} (U_i e^{-\gamma x} - U_r e^{\gamma x}) \end{cases} \quad (2)$$

式中: U_i 为电缆的正向传播电压; U_r 为电缆的反向传播电压; γ 和 Z_0 分别为电缆的传播常数和特征阻抗,其计算公式为:

$$\begin{cases} \gamma(\omega) = \sqrt{(R+j\omega L)(G+j\omega C)}, \\ Z_0 = \sqrt{\frac{R+j\omega L}{G+j\omega C}} \end{cases} \quad (3)$$

另外,电缆的传播常数可进一步写为:

$$\begin{cases} \gamma(\omega) = \alpha + j\beta, \\ v = \frac{\omega}{\beta} = \frac{2\pi f}{\beta} \end{cases} \quad (4)$$

式中, α 为衰减常数, β 为相移常数, v 为电磁波在电缆中的波速。

1.2 基于双端电流的早期故障定位原理

当电缆产生早期电弧故障时,故障点会向线路两侧同时产生大小相同、方向相反的电弧脉冲信号,并且在遇到其余缺陷位置时,行波信号会产生折反射现象,早期电弧故障行波传输如图 2 所示。

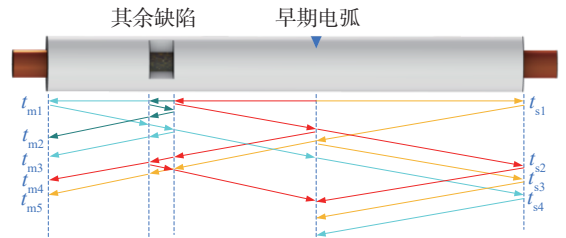


图2 电弧行波传输

Fig. 2 Arc traveling wave transmission

根据图 2 所示,由于行波在缺陷位置的折反射,在以单端行波进行缺陷定位时,容易造成行波来源的误判,最终影响故障定位结果。考虑行波信号从故障点首次传输至电缆两端的时间受缺陷影响较小,因此可以通过双端行波测量实现对早期电弧故障的定位。

假设电缆长度为 l ,早期电弧故障位置距离首端为 x ,电弧行波的波速为 v ,行波首次传输至电缆首末端的时间分别为 t_{m1} 和 t_{s1} ,则有:

$$\begin{cases} l - x = vt_{s1}, \\ x = vt_{m1} \end{cases} \quad (5)$$

则电缆故障位置为:

$$x = \frac{l - v(t_{s1} - t_{m1})}{2} \quad (6)$$

由于电缆早期电弧为接地电弧故障,因此,在电缆两端接地线位置分别放置电流互感器,通过监测电弧首次传输至电缆两端的电流行波时间差实现早期故障定位。

2 基于伪魏格纳分布(PWVD)与时频互相关的行波时延估计

通常,基于电流时域信号的故障定位需要有较高的时域采样率,并且其波容易遭受环境噪声的影响。考虑电缆离线定位技术的时频域反射法,可从时频域角度对信号进行分析,具有较高的定位精度,因此本文从时频域角度对双端采集电流信号进行分析,以获取准确的行波传输时延来实现对故障位置计算^[22-23]。

魏格纳分布(WVD)算法使用时间和频率的联合函数来描述信号的能量密度随时间的变化情况^[24],因此可以对双端电流信号同时使用WVD算法,并以双端信号能量密度最大位置的时间延迟判断故障位置。对于信号 $s(t)$ 的WVD算法的计算公式为:

$$W_z(t, \omega) = \int_{-\infty}^{\infty} s\left(t + \frac{\tau}{2}\right) s^*\left(t - \frac{\tau}{2}\right) e^{-j\omega\tau} d\tau \quad (7)$$

式中, $s^*(t)$ 为 $s(t)$ 的共轭函数, t 为时间, τ 为时延。信号的时频分布图如图3所示。

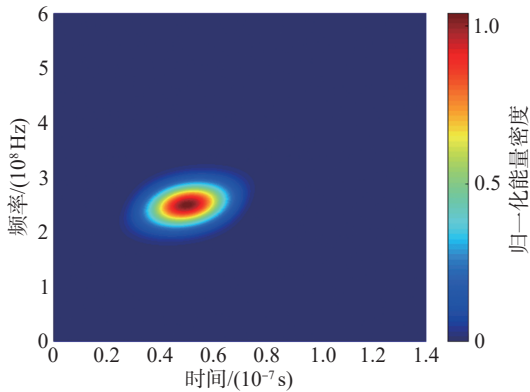


图3 信号的时频分布

Fig. 3 Time-frequency distribution of signal

但当信号存在多个分量时,WVD算法会产生明显的交叉项干扰。因此,考虑电弧放电信号有较宽的频率分量^[25],在研究电流信号的时频分布时需要将能量较低部分进行一定程度的抑制。

伪魏格纳分布(PWVD)算法与平滑伪魏格纳分布(SPWVD)算法均通过加窗方式对交叉项进行一定程度抑制,但SPWVD算法由于采用平滑处理,其空间分辨率要小于PWVD算法^[23],因此本文选用PWVD算法对信号进行时频处理。PWVD算法的计算公式为:

$$W_z(t, \omega) = \int_{-\infty}^{\infty} s\left(t + \frac{\tau}{2}\right) s^*\left(t - \frac{\tau}{2}\right) h(\tau) e^{-j\omega\tau} d\tau \quad (8)$$

式中, $h(\tau)$ 为窗函数。对于常用的窗函数形式,考虑Hanning窗对主频能量具有十分优秀的集中能力,并且对次频能量具有良好的衰减速度^[26],因此选取加Hanning窗的PWVD算法进行时频分析。

在计算双端电流信号的时频分布后,需要对二者信号的时间延迟进行分析。时频互相关函数 $C_{ms}(\tau)$ 从时频域角度对信号进行相似性计算,根据最大相似性发生的位置可以对信号进行时延估计^[27],时频互相关函数 $C_{ms}(\tau)$ 计算公式如下:

$$C_{ms}(\tau) = \frac{2\pi}{E_m E_s(\tau)} \int_{t=\tau-T_s}^{t=\tau+T_s} \int_{-\infty}^{+\infty} W_s(t, \omega) \cdot W_m(t - \tau, \omega) d\omega dt \quad (9)$$

式中: $W_m(t, \omega)$ 和 $W_s(t, \omega)$ 分别为传输电缆首末端电流信号的时频分布 T_s 为时间半窗长度; E_m 和 E_s 分别为首末端信号的时频域能量,其计算公式为:

$$\begin{cases} E_s(\tau) = \int_{t=\tau-T_s}^{t=\tau+T_s} \int_{-\infty}^{+\infty} W_s(t, \omega) d\omega dt, \\ E_m(\tau) = \int_{-T_s}^{T_s} \int_{-\infty}^{+\infty} W_m(t, \omega) d\omega dt \end{cases} \quad (10)$$

基于以上分析,在电缆两端分别设置电流互感器采集电弧脉冲传输至两端的电流行波,并使用加Hanning窗的PWVD算法对二者信号进行时频分布计算,最终通过时频互相关函数求取两信号的时间延迟,并计算早期故障位置。

3 仿真实验

3.1 电缆早期故障模型

对于电缆的早期故障,通常使用恒定电阻串联非线性电阻的形式进行模拟,常用的电弧模型有Mayr、Cassie、Habedank模型等^[28-29]。其中,文献[28]基于电弧的Mayr模型,通过对电弧电阻及剩余功率的波形进行分析,提出“电弧高阻值持续时间(DUR,记为 t_{dur})、最大电弧电阻出现时间(OFS,记为 t_{ofs})、最大电弧电阻值(EXT,记为 R_{ext})”3个参数实现对电弧模型的更精准表征。电弧电阻 R_{arc} 表达式为:

$$\ln(R_{arc}(t_d)) = \left(\frac{T}{8} - \frac{t_{dur}}{4}\right) \cdot m \cdot b_1 + \ln(R_{ext}) \quad (11)$$

式中:中间变量 $b_1 = 4\ln(R_{ext})/t_{dur}$; t_d 为半周期中 R_{arc} 首次到达最大值的时间,由 t_{ofs} 进行调节; T 为电弧电阻的周期; m 为常数。

基于式(11),在PSCAD/EMTDC仿真软件中搭建了图4所示的10 kV电缆的早期故障线路。

图4中,电缆A段与电缆B段具有相同的结构参数以及电气参数,通过改变两段电缆长度可以对早期故障位置进行调整,其电缆结构参数及电气参数如表1所示。

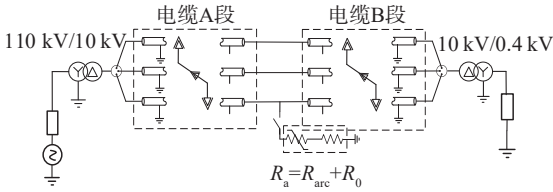


图 4 电缆早期故障模型

Fig. 4 Cable incipient fault model

表 1 电缆结构参数及电气参数

Tab. 1 Cable structure parameters and electrical parameters

结构	(外)半径/mm	电阻率/($\Omega \cdot m$)	相对介电常数
缆芯	6.5	2.826×10^{-8}	
绝缘层	12.0		2.3
屏蔽层	13.0	1.724×10^{-8}	
外护套	15.0		8.0

在设定 t_{dur} 为 0.006 136 s, t_{ofs} 为 0.12 s, T 为 0.02 s, R_{ext} 为 2 000 Ω , R_0 为 100 Ω 时, 得到图 5 所示早期电弧故障的电压波形。

由图 5 所示的电压波形可知, 当电缆中产生早期电弧故障时, 故障区电压波形呈马鞍状, 并且电弧出现在电压相位的 $60^\circ \sim 120^\circ$ 之间, 因此可以判定此时产生了早期电弧故障。

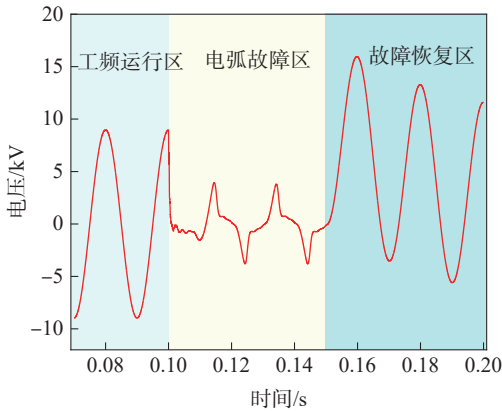


图 5 早期故障电压波形

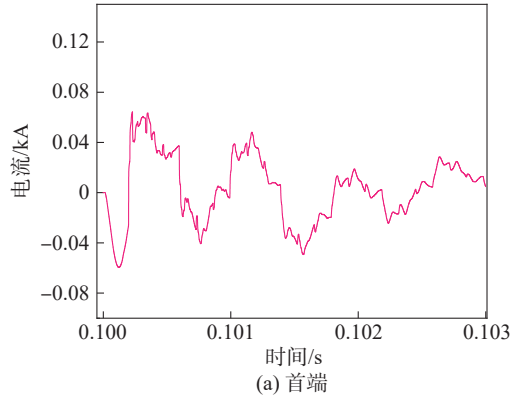
Fig. 5 Incipient voltage waveform

3.2 本文早期故障定位方法验证

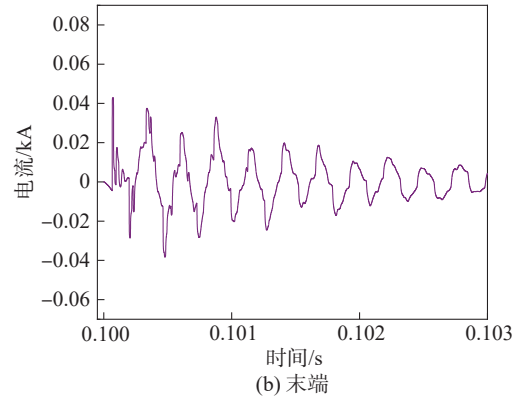
基于图 4 建立的电缆早期故障模型, 设定电缆 A 段为 3 km, 电缆 B 段为 1 km, 在采样率为 20 MHz 时, 测得电缆首末端接地电流波形如图 6 所示。

通过对电缆首末端电流进行加 Hanning 窗的 PWVD 算法处理, 得到图 7 所示的首末端电流信号的时频分布情况。

由图 7 可知, 由于传输时间的不同, 双端电流信号的时频分布位置会存在差异。同时, 观察图 7(b) 发现, 其时频分布图中存在多个位置的能量聚集, 这是由于早期故障位置距离末端较近, 电弧脉冲在电缆末端与故障位置间的多次折反射导致, 但是行波的多次折反射以及远距离传输衰减会导致信号的能量密度降低。



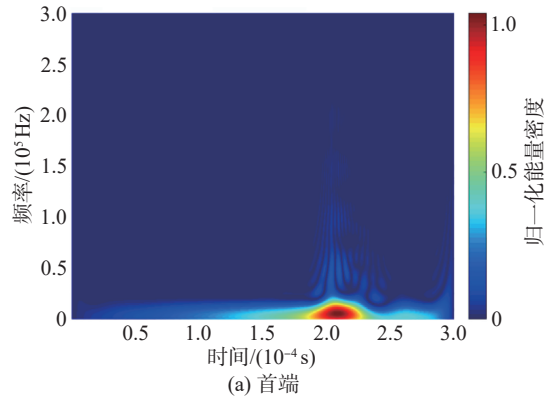
(a) 首端



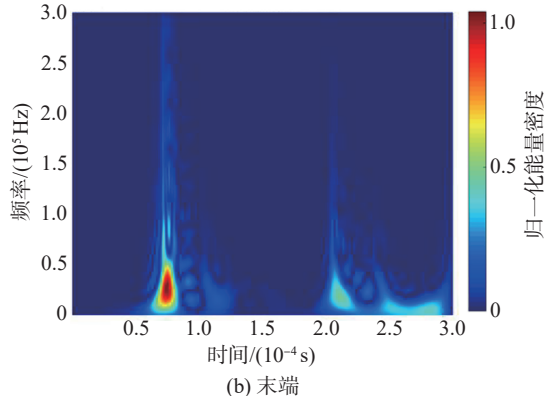
(b) 末端

图 6 首末端电流波形

Fig. 6 Head and end current waveform



(a) 首端



(b) 末端

图 7 首末端电流时频分布

Fig. 7 Time-frequency distribution of head and end current

根据式 (9) 与 (10) 可知, 时频互相关函数在计算信号的相似性时, 会同时考虑信号的时频位置及能量

密度,因此多次折反射信号并不会对时频互相关结果造成影响。首末端电流信号的时频互相关曲线如图8所示。

由图8可知,由于电弧脉冲具有较宽的频段范围,因此信号在此区间内均具有较高的时频互相关幅值。在 $10.9\ \mu\text{s}$ 位置出现了时频互相关幅值的最大值,因此将其作为电弧脉冲传输至电缆首末端电流信号的时间延迟。

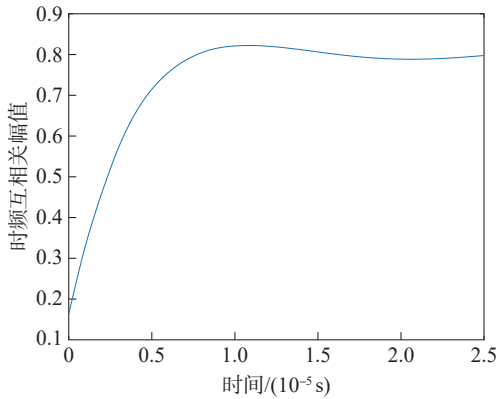


图8 首末端信号时频互相关结果

Fig. 8 Time-frequency cross-correlation results of head and end signals

在获取电弧脉冲传输至电缆两端的传输时延后,还需对电弧脉冲的波速进行计算。根据图7中信号的时频分布结果,选取能量密度最大位置的频率作为电弧的中心频率,并结合表1中电缆的结构参数及电气参数,通过式(1)~(4)计算波速,在中心频率为 $20\ \text{kHz}$ 时,计算得到电弧的波速为 $187.65\ \text{m}/\mu\text{s}$ 。

根据上述电弧波速并通过式(6)可将图8中的时间坐标转换为故障距离坐标,并得到图9所示的电缆早期故障定位结果。

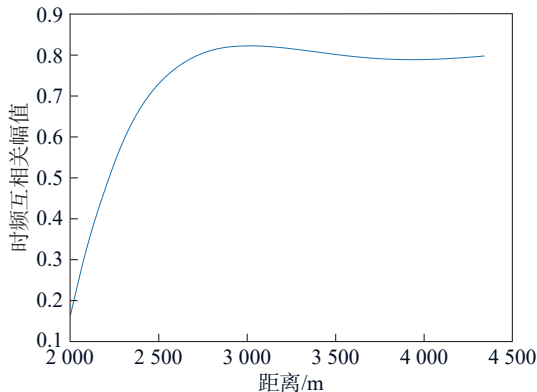


图9 电缆早期故障定位结果

Fig. 9 Cable incipient fault location results

由图9可见,在 $3\ 022.71\ \text{m}$ 位置出现了时频互相关幅值的最大值,此时计算电缆的早期故障定位误差为 0.57% ,说明本文方法具有较高的定位精度。

3.3 噪声干扰对定位精度影响

为研究噪声干扰对定位精度的影响,对采集的双端电流信号添加不同程度的白噪声。分别设置信噪比(SNR)为 80 、 50 和 $30\ \text{dB}$,以首端电流波形为例,不同SNR下的首端电流波形如图10所示。

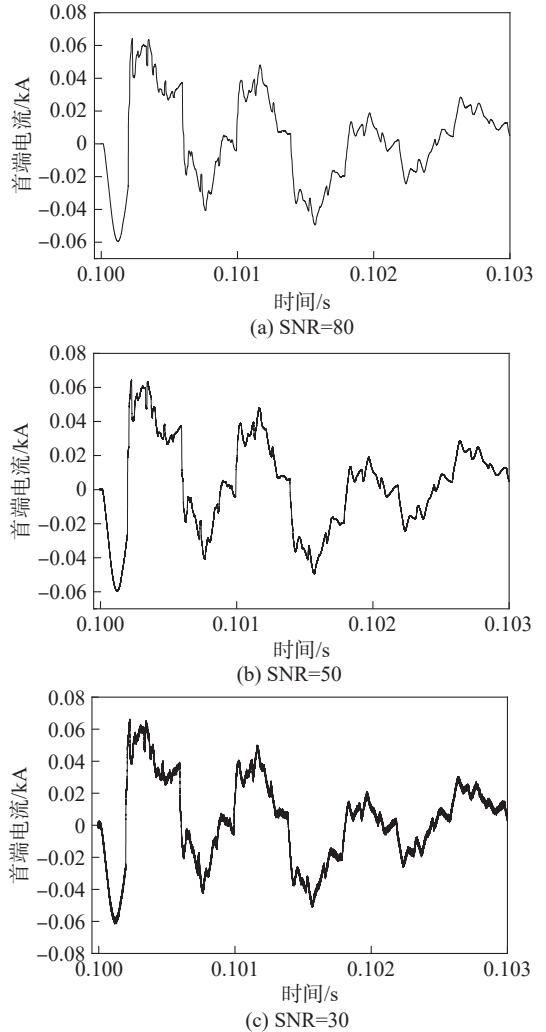


图10 不同SNR下首端电流波形

Fig. 10 Head current waveforms at different SNR

通过对不同SNR的电流信号进行PWVD计算,发现信号的时频分布并未产生较大变化,其中,SNR为 $30\ \text{dB}$ 时电缆的首末端电流信号时频分布结果如图11所示。

对比图11与7,当信号的SNR减小时,由于噪声的影响,其时频分布产生了小幅度扩散,但是并未影响能量密度较大位置的分布情况。对不同SNR时的首末端电流进行故障定位分析,得到图12所示结果。

由图12可知,在SNR分别为 80 、 50 、 $30\ \text{dB}$ 时,采用本文方法计算得到的故障位置分别为 $3\ 027.21$ 、 $3\ 043.73$ 和 $3\ 083.69\ \text{m}$,定位误差分别为 0.68% 、 1.09% 和 2.09% ,由此说明了本文方法的可行性。

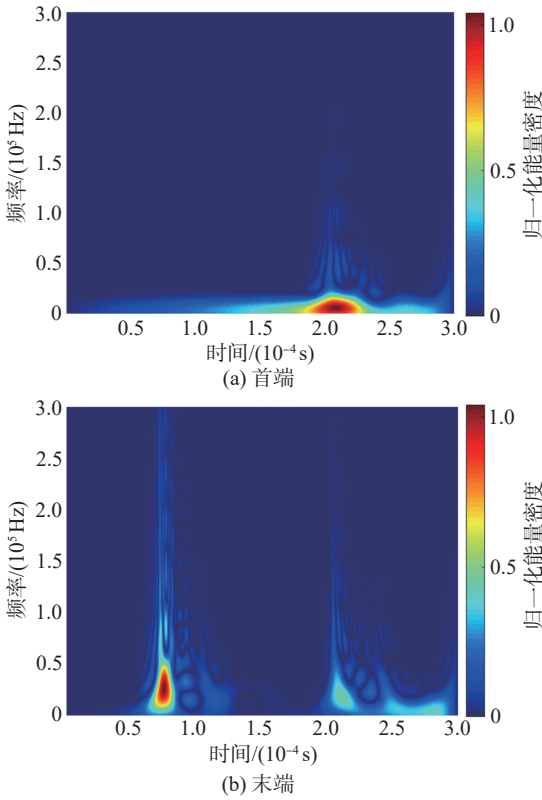


图 11 SNR=30时的首末端电流时频分布

Fig. 11 Time-frequency distribution of the head and end current when SNR=30

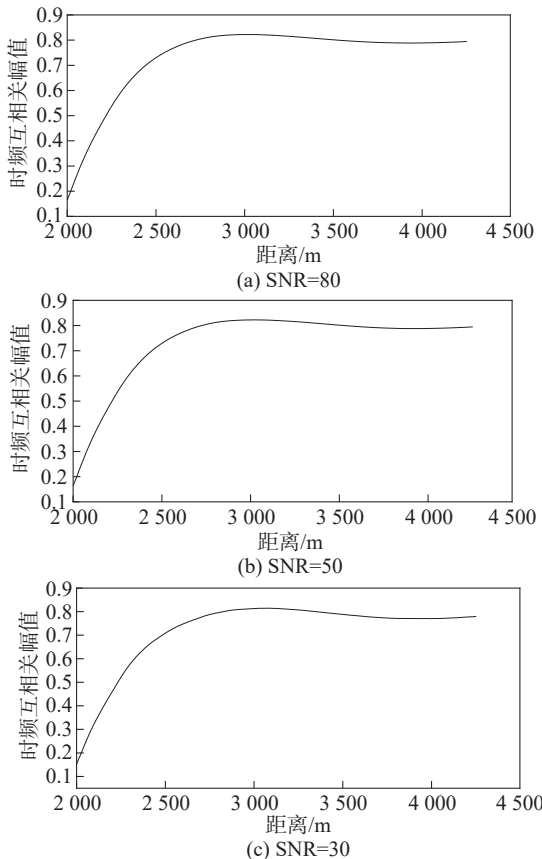


图 12 不同 SNR 下故障定位结果

Fig. 12 Fault location results under different SNR

4 实验验证

为验证本文方法在电力电缆早期故障中的定位效果,搭建 105 m 10 kV 电缆早期故障测试平台,包括调压箱、变压器、水阻、测试电缆、示波器,以及电流互感器。其中电缆的结构参数与表 1 相同,在 25 m 中间接头位置制作遭受潮气的刀痕缺陷来模拟电缆早期故障,测试平台如图 13 所示。

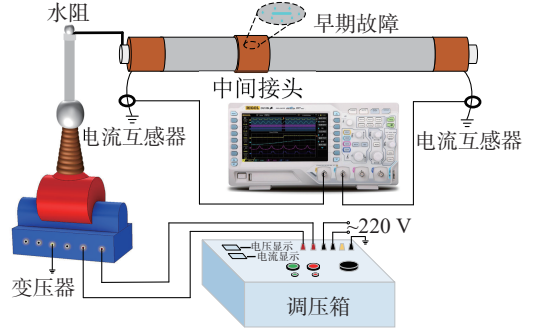


图 13 电缆早期故障测试平台

Fig. 13 Cable incipient fault test platform

通过调压箱、变压器产生工频高压用于激发电缆电弧故障,电流互感器采集传输至电缆两端的接地电流,并传输至示波器进行显示与存储。考虑到电缆长度远小于实际线路中电缆长度,并且电弧传输至电缆两端时间极短,因此在实验中使用较高的采样率来保证足够的定位精度。设置采样率为 500 MHz,当电缆产生早期故障时,其两端电流波形如图 14 所示。

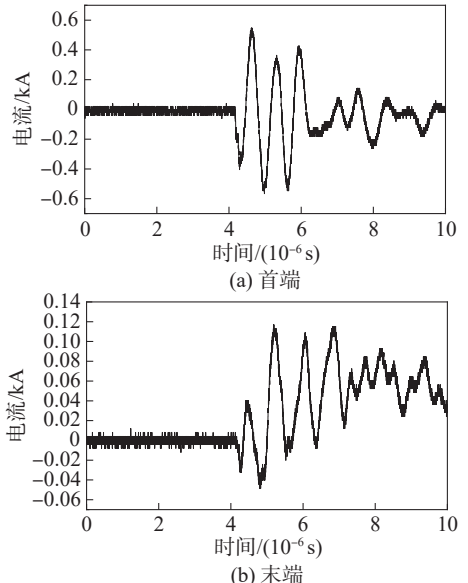


图 14 电缆首末端电流测试结果

Fig. 14 Cable head and end current test results

通过对其使用加 Hanning 窗的 PWVD 算法处理,并且进行时频互相关计算及坐标转换,得到图 15 所示的电缆早期故障定位曲线。

由图 15 可知,在电缆的 30.63 m 处出现了时频互

相关幅值的最大值,以此位置作为电缆早期故障位置时,其定位误差为5.36%。考虑到实验中电缆长度较短,电弧脉冲在采样周期内产生了多次折反射信号的叠加,并且电弧在短距离传输时能量衰减较小会造成定位精度的下降。但是,综合第3节仿真与第4节实验结果,基本可以说明本文方法具有较高的定位精度。

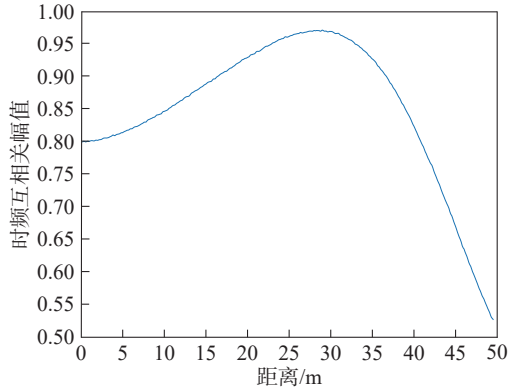


图15 早期故障定位实验结果

Fig. 15 Experimental results of incipient fault location

5 结论

基于行波传输理论,通过对电弧行波在电缆中的传输过程分析,建立了电缆早期故障的定位模型,提出了基于双端电流测量的早期故障定位方法。使用加Hanning窗的PWVD算法及时频互相关函数实现了电缆早期故障定位研究,其中,通过加Hanning窗的PWVD算法对信号进行时频域分析,能有效避免时域分析容易遭受噪声或者放电信号干扰导致的定位精度低的问题。通过仿真和实验的双重验证,证明了本方法具有较高的定位精度,并且具有较好的抗噪声干扰能力。

参考文献:

[1] Lu Guojun, Xiong Jun, Wang Yong, et al. 10 kV XLPE cable partial discharge detection based on oscillating waves[J]. Electric Power Automation Equipment, 2010, 30(11): 137–140. [陆国俊,熊俊,王勇,等.振荡波电压法检测10 kV电缆局部放电试验[J].电力自动化设备,2010,30(11):137–140.]

[2] Zhang Cheng, Li Hongfei, Yang Yanbin, et al. Research progress in ageing, evaluation, and rejuvenation of XLPE cable insulation[J]. Insulating Materials, 2020, 53(7): 1–11. [张成,李洪飞,杨延滨,等.交联聚乙烯电缆老化、诊断及修复研究进展[J].绝缘材料,2020,53(7):1–11.]

[3] Tang Zhirong, Xu Yefei, Zhou Kai, et al. A frequency sweep location method for soft faults of power cables based on MUSIC-pseudospectrum[J]. IEEE Transactions on Instrumentation and Measurement, 2023, 72: 3510410.

[4] 刘世涛,徐兆国,杨凯,等.典型缺陷下电力电缆局部放电特征与识别[J].高电压技术,2023,49(增刊):36–39.

[5] Kruizinga B, Wouters P A A F, Steennis E F. Fault development

upon water ingress in damaged low voltage underground power cables with polymer insulation[J]. IEEE Transactions on Dielectrics and Electrical Insulation, 2017, 24(2): 808–816.

[6] Li Feng, Xu Bingyin, Yan Tingchun. Modeling and simulating of arcs for cable fault location in ARM mode[J]. Automation of Electric Power Systems, 2014, 38(11): 104–108. [李峰,徐丙垠,颜廷纯.电弧反射法电缆故障测距中的电弧建模与仿真[J].电力系统自动化,2014,38(11):104–108.]

[7] Jannati M, Vahidi B, Hosseini S H. Incipient faults monitoring in underground medium voltage cables of distribution systems based on a two-step strategy[J]. IEEE Transactions on Power Delivery, 2019, 34(4): 1647–1655.

[8] Qu Ke, Zhang Wenhai, Zhang Shu, et al. Model-free underground cable incipient fault location using two-terminal zero-sequence measurements[J]. International Journal of Electrical Power & Energy Systems, 2022, 140: 108057.

[9] Qu Ke, Zhang Wenhai, Xiao Xianyong, et al. Condition monitoring for incipient faults of cable joint insulation based on waveform attenuation factor[J]. High Voltage Engineering, 2022, 48(1): 318–327. [瞿科,张文海,肖先勇,等.基于波形衰减因子的电缆接头绝缘早期故障状态监测[J].高电压技术,2022,48(1):318–327.]

[10] Liu Surong, Hu Yuxiao, Zheng Jiankang, et al. Dynamics simulation of 10 kV cable tunnel fire for single-phase arc grounding fault[J]. High Voltage Engineering, 2021, 47(12): 4341–4348. [刘素蓉,胡钰骁,郑建康,等.10 kV电缆单相电弧接地故障引燃隧道的火灾动态仿真[J].高电压技术,2021,47(12):4341–4348.]

[11] Zhou Zhengxiong, Xia Xiangyang, Zhu Peng, et al. Identification method for incipient intermittent arc ground fault of high-voltage cables[J]. Electric Power, 2020, 53(12): 167–176. [周正雄,夏向阳,朱鹏,等.高压电缆早期间歇性电弧接地故障识别方法[J].中国电力,2020,53(12):167–176.]

[12] Wang Ying, Sun Jianfeng, Xiao Xianyong, et al. Cable incipient fault classification and identification based on optimized convolution neural network[J]. Power System Protection and Control, 2020, 48(7): 10–18. [汪颖,孙建风,肖先勇,等.基于优化卷积神经网络的电缆早期故障分类识别[J].电力系统保护与控制,2020,48(7):10–18.]

[13] Yao Haiyan, Zhang Jing, Liu Yi, et al. Method of cable incipient faults detection and identification based on multi-scale wavelet criterions and time-frequency feature association[J]. Power System Protection and Control, 2015, 43(9): 115–123. [姚海燕,张静,留毅,等.基于多尺度小波判据和时频特征关联的电缆早期故障检测和识别方法[J].电力系统保护与控制,2015,43(9):115–123.]

[14] Liu Ning, Fan Bo, Xiao Xianyong, et al. Cable incipient fault identification with a sparse autoencoder and a deep belief network[J]. Energies, 2019, 12(18): 3424.

[15] Zhang Jianwen, Zhou Peng, Chen Huanxu. Simulation of

- transmission line single-phase ground fault location based on improved impedance method[J]. *Electrical Measurement & Instrumentation*, 2018, 55(3):84–87. [张建文, 周鹏, 陈焕桐. 基于改进阻抗法的单相接地故障测距仿真[J]. *电测与仪表*, 2018, 55(3):84–87.]
- [16] Zhang Wenhai, Xiao Xianyong, Zhou Kai, et al. Multicycle incipient fault detection and location for medium voltage underground cable[J]. *IEEE Transactions on Power Delivery*, 2017, 32(3):1450–1459.
- [17] Tang Zuoxin, Zhou Kai, Xu Yefei, et al. Frequency domain reflectometry cell average constant false alarm rate cable defect identification method considering attenuation compensation[J]. *Transactions of China Electrotechnical Society*, 2024, 39(16):5194–5205. [唐作鑫, 周凯, 徐叶飞, 等. 考虑衰减补偿的频域反射单元平均恒虚警率电缆缺陷识别方法[J]. *电工技术学报*, 2024, 39(16):5194–5205.]
- [18] Liu Yonghao, Cai Zexiang, Xu Min, et al. Single-end fault location algorithm based on traveling wave speed optimization and modal propagation time difference for DC transmission line[J]. *Electric Power Automation Equipment*, 2012, 32(10):72–76. [刘永浩, 蔡泽祥, 徐敏, 等. 基于波速优化与模量传输时间差的直流线路单端行波测距新算法[J]. *电力自动化设备*, 2012, 32(10):72–76.]
- [19] Shu Hongchun, Tian Xincui, Dong Jun, et al. A single terminal cable fault location method based on fault characteristic frequency band and TT transform[J]. *Proceedings of the CSEE*, 2013, 33(22):103–112. [束洪春, 田鑫萃, 董俊, 等. 利用故障特征频带和TT变换的电缆单端行波测距[J]. *中国电机工程学报*, 2013, 33(22):103–112.]
- [20] Antonini G, Orlandi A, Pignari S A. Review of clayton R. Paul studies on multiconductor transmission lines[J]. *IEEE Transactions on Electromagnetic Compatibility*, 2013, 55(4):639–647.
- [21] Tang Zhirong, Zhou Kai, Meng Pengfei, et al. A frequency-domain location method for defects in cables based on power spectral density[J]. *IEEE Transactions on Instrumentation and Measurement*, 2022, 71:9005110.
- [22] Yin Zhendong, Wang Li, Chen Hongzhen, et al. Application of augmented time frequency domain reflectometry in detection of complex cable faults[J]. *Proceedings of the CSEE*, 2020, 40(23):7760–7772. [尹振东, 王莉, 陈洪圳, 等. 增广时频域反射法在电缆复合故障检测中的应用[J]. *中国电机工程学报*, 2020, 40(23):7760–7772.]
- [23] Cao Yating, Zhou Kai, Meng Pengfei, et al. Cable defect location based on orthogonal matching pursuit and pseudo Wigner–Ville distribution[J]. *Transactions of China Electrotechnical Society*, 2023, 38(16):4489–4498. [操雅婷, 周凯, 孟鹏飞, 等. 基于正交匹配-伪魏格纳分布的电缆缺陷定位[J]. *电工技术学报*, 2023, 38(16):4489–4498.]
- [24] 张贤达. *现代信号处理*[M]. 2版. 北京:清华大学出版社, 2002.
- [25] Yang Qing, Qi Yue, Wei Siyu, et al. Electromagnetic radiation characteristics of overhead distribution line fault arc and their fault location application[J]. *Proceedings of the CSEE*, 2024, 44(1):353–361. [杨庆, 齐玥, 韦思宇, 等. 架空配电线路故障电弧的电磁辐射特性及故障定位应用[J]. *中国电机工程学报*, 2024, 44(1):353–361.]
- [26] Li Rong, Zhou Kai, Wan Hang, et al. Moisture location of 10 kV cable joints in medium voltage distribution grid based on frequency domain reflection[J]. *Power System Technology*, 2021, 45(2):825–832. [李蓉, 周凯, 万航, 等. 基于频域反射法的 10 kV 配电网电缆中间接头受潮定位[J]. *电网技术*, 2021, 45(2):825–832.]
- [27] Wang Yuhao, Zhou Kai, Wang Xianjin, et al. Power cable defects location based on improved time–frequency domain reflectometry[J]. *Proceedings of the CSEE*, 2021, 41(7):2584–2594. [王昱皓, 周凯, 汪先进, 等. 基于改进时频域反射法的电力电缆局部缺陷定位[J]. *中国电机工程学报*, 2021, 41(7):2584–2594.]
- [28] Wei Mingjie, Liu Weisheng, Shi Fang, et al. Distortion-controllable arc modeling for high impedance arc fault in the distribution network[J]. *IEEE Transactions on Power Delivery*, 2021, 36(1):52–63.
- [29] Wang Bin, Liang Chengguang, Li Fengting. Arc modeling and single-end fault location for arc grounding fault in transmission line considering arc gap length[J]. *Proceedings of the CSEE*, 2019, 39(4):1001–1009. [王宾, 梁晨光, 李凤婷. 计及间隙长度的弧光接地故障建模及单端测距[J]. *中国电机工程学报*, 2019, 39(4):1001–1009.]

Research on Incipient Fault Location of Cable Based on Double-ended Current Measurement

MENG Pengfei¹, LI Tengfei¹, WANG Wangang^{2*}, XIE Shijun³, ZHOU Kai¹, TANG Zhirong¹

(1. College of Electrical Engineering, Sichuan University, Chengdu 610065, China;

2. College of Physics and Engineering Technology, Chengdu Normal University, Chengdu 610130, China;

3. State Grid Sichuan Electric Power Research Institute, Chengdu 610041, China)

Abstract:

Objective The incipient fault of the cable occurs at the local insulation defect of the cable and constitutes an intermittent grounding arc fault. As the degree of cable insulation deterioration increases, the frequency of incipient faults continuously rises and eventually develops into a perma-

nent fault. At present, positioning methods for cable incipient faults primarily rely on the impedance method and the traveling wave method. The cable incipient fault location method, based on the impedance method, constructs the circuit equation using the fault voltage and the transmission current at the head end, and estimates the fault distance based on the purely resistive nature of the arc resistance and its corresponding parametric formula. However, this model does not consider the attenuation and dispersion of the arc current during transmission, resulting in a decrease in positioning accuracy. The incipient fault location method based on the traveling wave requires an analysis of electromagnetic traveling wave propagation in the cable, which determines the fault location by calculating the time difference in wave transmission. However, the single-ended traveling wave positioning method results in misjudgments due to refraction and reflection at the defect position. In addition, the traditional double-ended positioning method can inaccurately identify the wavefront position due to noise or discharge interference when analyzing the signal's time-domain information, affecting location accuracy. Therefore, based on two-terminal traveling wave measurements, this study proposes an accurate positioning method for cable incipient faults by calculating the time-frequency distribution of the signals.

Methods Initially, the distributed parameter model of high-frequency electromagnetic wave transmission in cables was analyzed. Considering the skin effect and proximity effect of the cable, the distributed parameters were modified and expressed, and the propagation constant and traveling wave velocity of the electromagnetic wave in the cable were calculated. Then, by analyzing the transmission process of electromagnetic waves and the multiple refraction and reflection phenomena at the defect location in the cable, the corresponding relationship between the cable fault location and the time difference between the first transmission of the arc traveling wave to both ends of the cable was obtained. After that, considering the influence of noise on the time domain signal, the signal was analyzed in the time-frequency domain. The WVD algorithm formed the basis of the time-frequency distribution algorithm. However, due to the presence of cross-term interference, the accuracy of the positioning results was affected. The Hanning window exhibited good concentration capability for the main frequency of the signal and demonstrated strong attenuation for the secondary frequency. Therefore, the PWVD algorithm, incorporating the Hanning window, was employed to calculate the time-frequency distribution of the signal. Simultaneously, when calculating the time delay of the two signals, the time-frequency cross-correlation function was utilized to determine the similarity of the time-frequency distribution, and the maximum value of the time-frequency cross-correlation amplitude was adopted as the transmission delay of the signal, enabling the identification of the fault location.

Results and Discussions For the above scheme, the positioning algorithm was first verified through simulation. Based on the arc resistance formula, the cable incipient fault model was constructed in PSCAD. The total cable length was set to 4 km, and the arc fault was introduced at a distance of 3 km from the head end. The ground current waveforms transmitted to both ends of the cable were collected, and the time-frequency distribution and time-frequency cross-correlation results of the currents were calculated. The maximum value of the time-frequency cross-correlation amplitude occurred at 10.9 μs , indicating that the transmission delay was approximately 10.9 μs . Then, the wave velocity of the arc was calculated based on the center frequency of the signal's time-frequency distribution. When the center frequency was 20 kHz, the arc wave velocity was calculated to be 187.65 m/ μs . After applying the formula transformation, the fault location result was 3 022.71 m, with a location error of 0.57%. The influence of noise on positioning accuracy was then examined. When the SNR of the current signals at both ends was set to 80, 50, and 30 dB, respectively, the positioning results were 3 027.21, 3 043.73, and 3 083.69 m, and the corresponding positioning errors were 0.68%, 1.09%, and 2.09%. The simulation effectively verified the algorithm's anti-noise capability. In the experimental validation, a 10 kV 105 m cable experimental platform was constructed, and the incipient fault was introduced at the 25 m position. Two current sensors were placed at both ends of the cable to collect the arc pulse. Due to the short cable length, the sampling rate was set to 500 MHz. At this setting, the incipient fault location of the cable was calculated to be 30.63 m, resulting in a positioning error of 5.36%. For the 105 m cable, the arc underwent multiple refractions in a very short time, affecting the accuracy of the positioning result; however, the outcome still demonstrated the feasibility of the proposed method.

Conclusions This study proposes an incipient fault location method for cables by analyzing the transmission process of arc pulses within the cable. The PWVD algorithm, combined with the Hanning window and the time-frequency cross-correlation function, is employed to calculate the fault location, effectively mitigating the issue of noise interference that typically affects time-domain signals. Simulation and experimental verification clearly demonstrate that the proposed method achieves high positioning accuracy and exhibits strong resistance to noise.

Key words: cable incipient fault; traveling wave transmission; two-terminal current; pseudo Wigner-Ville distribution; time-frequency cross-correlation

(编辑 赵 婧)

引用格式: Meng Pengfei, Li Tengfei, Wang Wangang, et al. Research on incipient fault location of cable based on double-ended current measurement[J]. *Advanced Engineering Sciences*, 2025, 7(4): 269–277. [孟鹏飞, 李腾飞, 王万岗, 等. 基于双端电流测量的电缆早期故障定位研究[J]. *工程科学与技术*, 2025, 57(4): 269–277.]